Polym. Bull. (2015) 72:2503–2518
DOI 10.1007/s00289-015-1415-3

ORIGINAL PAPER

Preparation and characterization of polyaniline-poly(styrene-acrylate) composite latexes

Fangfang Yang[1] · **Aiping Zhu**[1]

Received: 27 March 2014 / Revised: 4 April 2015 / Accepted: 30 May 2015 /
Published online: 9 June 2015

Abstract In this paper, poly(styrene-acrylate) latex with phosphate functional group (SA-PO) was prepared using mini-emulsion polymerization. Polyaniline (PANI) bonded SA (PANI-SA) composite was then prepared by in situ chemical oxidation polymerization of aniline. FT-IR and UV–Vis spectra confirm the formation of the PANI-SA composite. Small spherical particles of 10–20 nm in diameter on the surface of SA latexes are observed by SEM. DSC and TGA results indicate that there are chemical bonds formed between PANI and SA, and PANI in the PANI-SA composite can increase the glass transition temperature (T_g) and thermal decomposition temperature (T_d) of SA latex film effectively. Mechanical property testing indicates that PANI in PANI-SA composite can increase the mechanical properties of SA latex film. EIS measurements show that PANI in SA-PANI can significantly improve the corrosion resistance performance of waterborne SA coating. Compared with PANI/polymer composite system, PANI-SA has two advantages: avoidance of the aggregation problem of nanoscale PANI in polymer matrix and improvement of the interface adhesion between PANI and polymer matrix.

Keywords Poly(styrene-acrylate) (SA) latex · Mini-emulsion polymerization · In situ chemical oxidation polymerization · PANI

✉ Aiping Zhu
apzhu@yzu.edu.cn

[1] College of Chemistry and Chemical Engineering, Yangzhou University, Yangzhou 225002, People's Republic of China

Introduction

In recent years, considerable attention has been paid to organic conducting polymers such as polypyrrole, polyaniline (PANI) and polythiophene because they exhibit metallic-like conductivity [1–3]. Since PANI has outstanding features of oxidation–reduction quality, environmental protection, simple preparation technology and the advantages of cheap raw materials, it has great potential in the field of antifouling, antistatic coatings and anti-corrosion coatings [4–10]. The anti-corrosion mechanism of PANI has also been sufficiently studied as a green and long-term corrosion resistance auxiliary reagent [11–16]. In 1983, Mengoli conducted a series of research about electrochemical synthesis of PANI on sheet iron in alkaline solution in the presence of ammonium sulfate and aniline; ultimately he found that the membrane presented excellent corrosion resistant performance for about 80 h [17]. However, on account of the π-bonded macromolecular chain structure, conducting polymers such as PANI have larger rigidity, almost infusibility and insolubility, strong film brittle and poor mechanical properties [18–21]. Taking these factors into consideration, researchers have investigated PANI composite with thermoplastic polymers as matrix materials to improve machining performance of PANI.

There are many reports about the preparation and characterization of nano-PANI composite [21–26]. Most of the research shows that nanoscale PANI inevitably forms a state of aggregation in matrix polymers due to the surface and interface effect between nano-PANI and polymer matrix. This will affect anti-corrosion, conductivity and antifouling performance. Wang et al. have prepared epoxy resin composite in addition to organic phosphate doped PANI particles (PANI-OP) by blending. Having the amount of PANI-OP added range from 0.1 to 1 % can significantly improve the corrosion resistance of waterborne epoxy resin coating. However, with the increase in PANI-OP content, the aggregation exacerbated. This reduced the density and made the coating porous, resulting in poor corrosion resistance [27]. Cao et al. have acquired organic macromolecular anion acid doped PANI and dissolved it in ordinary solvent such as dimethyl benzene, making PANI blending processing possible [28, 29]. Talo et al. have applied this blending method to PANI/epoxy system, and found it demonstrates good corrosion resistance [30]. However, the solvent used in the process will cause serious pollution to the environment, which may restrict the application of the PANI blending system. When faced with these problems, most investigators focus on increasing the stability of PANI dispersion and controlling the size and morphology of particles to modulate the properties of PANI composites [31–33].

This paper proposes a novel approach to prepare poly(styrene-butylacrylate) (SA)-PANI composite with good interface adhesion in order to improve the consistency of PANI in matrix material and achieve the application of PANI in water-based metal anti-corrosion field. First of all, SA latexes containing phosphate groups (SA-PO) were prepared with mini-emulsion polymerization [34, 35]. This was followed by the chemical oxidation polymerization of aniline on the surface of SA latexes, driven by the electronic interaction between the phosphate groups on

SA latexes and aniline molecules. PANI-SA latexes composite with chemical bonds between phases can be obtained successfully from this process.

Materials and methods

Materials

Styrene and aniline (AR, Shanghai Chemical Reagent Co.) were purified by distillation under reduced pressure. Ammonium persulfate (APS) was purified by recrystallization in water. Sodium dodecyl sulfate (SDS), emulsifier OP-10, butyl acrylate, phosphate ester functional monomer (PAM 200), azodiisobutyronitrile (AIBN), hexadecane (HD) and hydrochloric acid (HCl, AR, Nanjing Chemical Reagent Co.) were used as received. Distilled water was used for all polymerization and treatment processes.

Synthesis

Preparation of styrene-acrylate (SA) latex with phosphate group (SA-PO)

A three-necked round bottom flask was filled with 20 g water, 0.2 g SDS, 2 g OP-10, 16.7 g styrene, 8.3 g butyl acrylate, 1.0 g PAM 200, 0.4 g hexadecane, and 0.55 g AIBN (initiator) and stirred for 0.5 h to form an emulsion. This emulsion was transferred to a homogenizer at 20,000 r/min for 10 min to form a mini-emulsion. The mini-emulsion polymerization took place in nitrogen atmosphere at 68 °C for 6 h to obtain SA-PO.

Preparation of PANI bonded SA latexes (PANI-SA)

SA-PO latexes (100 g) and aniline (valuable) were added into the three-necked round bottom flask with stirring under nitrogen atmosphere. HCl (36 %) was added dropwise into the above system to adjust the pH to 2. APS (initiator for oxypolymerization) solution was then added dropwise into the reaction system (the molar ratio of aniline monomer to APS was 1). The reaction took place in an ice bath for 24 h. The formulation of PANI-SA latexes with different content of PANI is listed in Table 1.

Table 1 Formulation of PANI-SA latexes with different content of PANI

	PAM 200 in SA (wt%)	Aniline monomer	SA polymer	Theoretically maximum PANI loading in SA (wt%)
SA-PO	4	0	25	0
PANI-SA-01	4	0.25	25	1
PANI-SA-02	4	0.5	25	2
PANI-SA-03	4	1	25	4
PANI-SA-04	4	2	25	8

Characterization

The morphology of the SA-PO and PANI-SA latexes was observed with a scanning electron microscope (SEM) using an S-4800 instrument (Hitachi Co., Japan) operated at an accelerating voltage of 15 kV (samples sputter coated with gold prior to examination). FT-IR analysis was performed with a Bruker VECTORTM 22 spectrometer (Bruker Co., Germany). Latex size and particle size distribution were determined by a dynamic light scattering (DLS) system (DLS-5022F, Brookhaven Instruments Co.) with a 500 W helium–neon laser of 660 nm wavelength at 25 °C. The oxidation state and the formation of polaron band were identified by UV–Vis spectroscopy (Cary 5000). A differential scanning calorimeter (DSC, NETZSCH DSC-204F1, Germany) was used to obtain the Tg of SA-PO and PANI-SA. The sample (about 5 mg) was first heated to 90 °C from −30 °C at a rate of 10 °C min^{-1}. Thermogravimetric analysis (TGA) was conducted with a Pyris 1 TGA instrument (Perkin Elmer Co., USA) at a heating rate of 20 °C per min in N_2 from room temperature up to 600 °C. Tensile properties of the samples were determined by an Instron Mechanical Tester (ASTM D638) at a crosshead speed of 50 mm/min at Stretching mode. All values reported here represent an average of the results for tests run on three specimens at room temperature. Corrosion protection property of coating with a 0.1 mm thickness was determined by electrochemical impedance spectroscopy (EIS) (Gamry Instrument potentiostat G750) in 3.5 % NaCl solution. A three-electrode cell was used with a working electrode with an exposed area of about 2 cm^2, reference calomel electrode and a platinum counter electrode. Gamry Instrument EIS300 Software measured the impedance in a frequency range of 0.01 Hz to 10^4 or 10^5 Hz by applying an AC voltage with amplitude of 10 mV around the corrosion potential. The measurements were performed as a function of immersion time.

Results and discussion

Synthesis of SA-PO and PANI-SA

As shown in Scheme 1a, PAM 200 is a monomer with the groups of phosphate monoester, phosphate diester and a small amount of phosphoric acid. After the mini-emulsion polymerization, the SA latexes with $-PO_4^{3-}$ (SA-PO) have been successfully prepared (Scheme 1b). In a strong acid environment, aniline is protonated since it has a p*K*a of 4.36 [36]. The protonated aniline is absorbed onto the SA-PO latex surface through electrostatic interaction with the phosphate groups. The chemical oxidation polymerization of aniline on the surface of SA latexes took place after the addition of APS. PANI-SA latexes composite can be obtained successfully as a result of this procedure (Scheme 1c).

The advantages of this method are: (1) PANI can uniformly form on the SA latex surface, thus avoiding clustering of the PANI in the composite material; (2) there are chemical bonds formed between PANI and SA latex matrix, which can improve the interface adhesion effectively; (3) PO_4^{3-} functional group can improve the wet

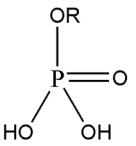

Phosphate Mono-ester

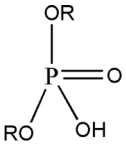

Phosphate Di-ester

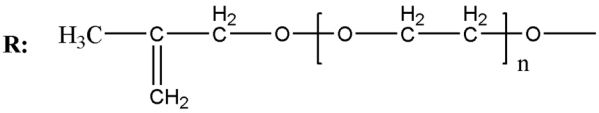

(a) Molecular structure of PAM 200

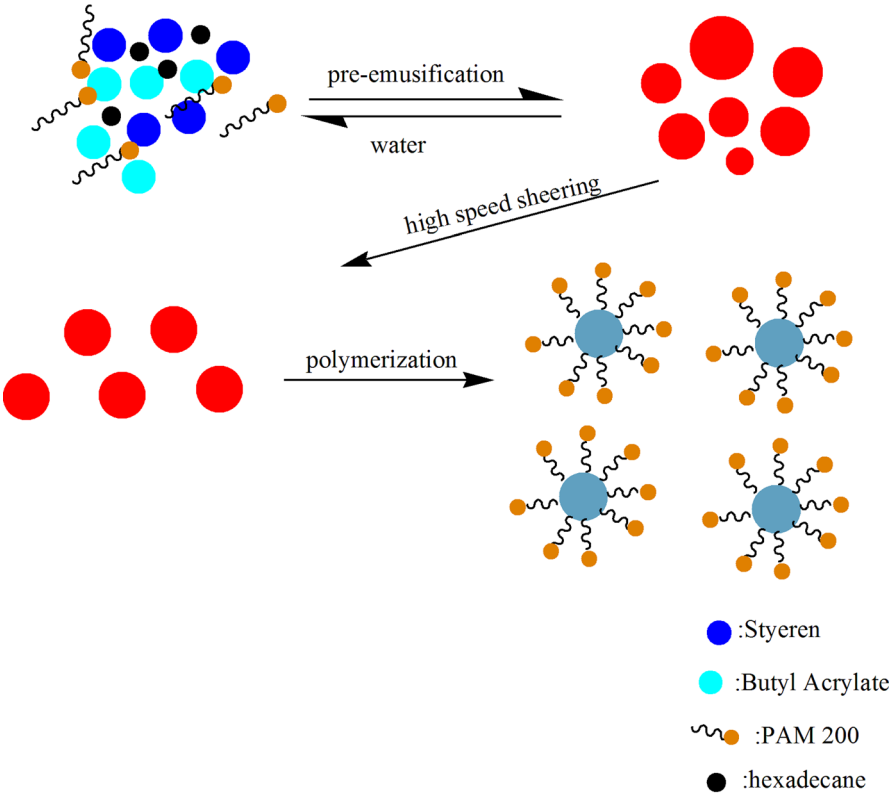

(b) Synthetic process of SA-PO

Scheme 1 Synthesis scheme of PANI-SA latexes: **a** molecular structure of PAM 200, **b** synthetic process of SA-PO, **c** synthetic process of PANI-SA

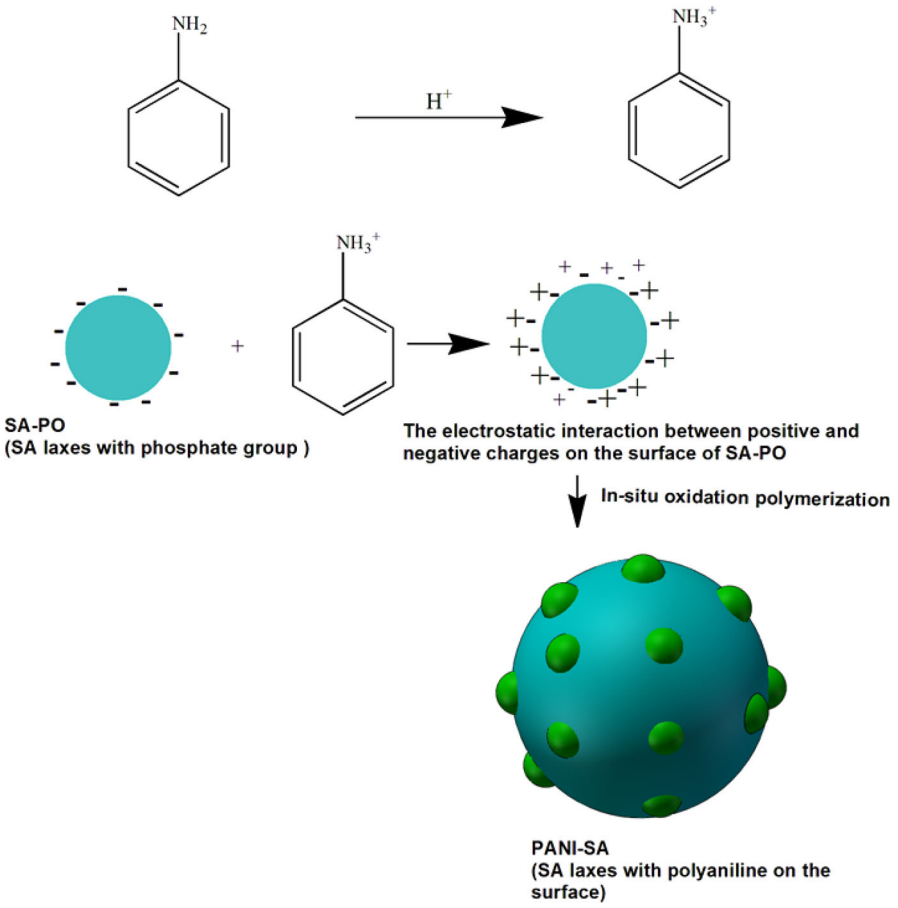

(c) Synthetic process of PANI-SA

Scheme 1 continued

adhesion of the coating on the metal surface and act as the slow corrosion agent for metal.

FT-IR

Figure 1 shows the FT-IR spectra of SA-PO and PANI-SA-02 latexes. As seen from the spectrum of SA-PO, the peaks at 2924 and 2864 cm^{-1} are attributed to the stretching vibration of $–CH_3$ and $–CH_2–$; the peak at 1733 cm^{-1} belongs stretching vibration of C=O; the peaks at 1237, 1167 cm^{-1} are symmetric stretching vibration of C–O–C, the peak at 707 cm^{-1} is attributed to the characteristic vibration of benzene. As seen from the spectrum of PANI-SA, besides the above characteristic peaks of SA-PO, the extra strong absorption peaks at 825, 1635, 1310, and 3387 cm^{-1} appeared and correspond respectively to the C–H bending vibration of

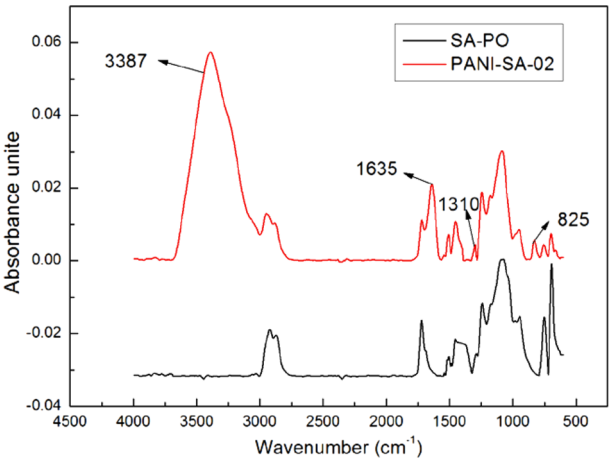

Fig. 1 FT-IR spectra of SA-PO and PANI-SA-02

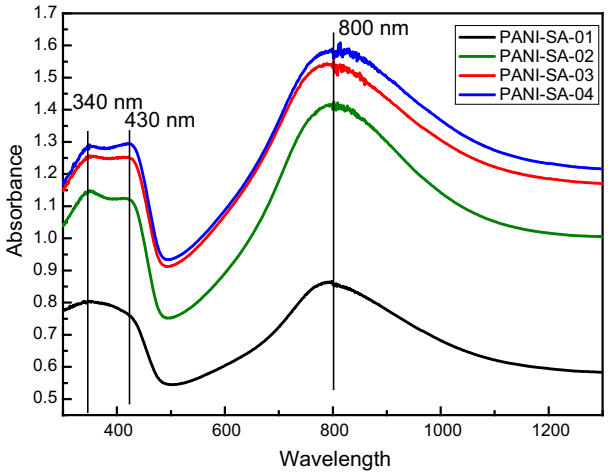

Fig. 2 UV–Vis spectra of SA-PO and PANI-SA

the *para* substituted benzene, mode vibration of quinone imine (N=Q=N), stretching vibration of C–N, and stretching vibration of N–H [37]. These results confirm the formation of PANI-SA composite latexes.

UV–Vis spectra

During the in situ chemical oxidation polymerization of aniline, the color of the system varies with the increase of aniline conversion. PANI-SA with low PANI content appears light green and PANI-SA with high PANI content demonstrates dark green. The color of PANI-SA indicates that PANI in PANI-SA is in its doped state (oxidation–reduction state) [38]. The UV–Vis spectrum (Fig. 2) was used to verify the doped state. It is well known that there are two peaks of PANI; one peak

at 340 nm is due to $\pi \rightarrow \pi^*$ transition of benzenoid ring and the other peak at 630 nm corresponds to the excitation of quinoid ring [39]. In the UV–Vis spectra, PANI-SA appears beside the peak of 340 nm, the two new peaks appear at 430 and 800 nm, respectively, indicating the formation of delocalized polarons [40]. After comparing the spectra of PANI-SA with different PANI content, it can be noted that the intensity of the peak at 800 nm increases remarkably with the increase of PANI content. Moreover, in the case of PANI-SA-01 (1 wt% PANI content) the polaron band at 800 nm blue shifts to 790 nm. This precisely indicates the reduction of the conjugation length. This may be assigned to the low PANI concentration bonding, resulting in the low molecular weight of PANI and most of the particles being left uncoated with PANI [41]. The spectra of PANI-SA composites confirm that PANI remains in its doped state in this composite system, which benefits the use of PANI-SA as a green and long-term corrosion resistance auxiliary reagent.

Morphology, size and size distribution

Figure 3 shows an SEM image of SA-PO latexes. It can be seen that SA-PO latexes show regular spherical morphology and its diameter ranges from 50 to 200 nm. Figure 4 shows the particle size and distribution as measured by DLS, which indicates that SA-PO latexes demonstrate a relatively broad size distribution from 50 to 250 nm. This may arise from the low reaction temperature and long nucleation period of the mini-emulsion polymerization.

Figure 5 shows SEM images of PANI-SA latexes. The surface of SA-PO is covered with uniformly dispersed, small PANI particles that are 10–20 nm in diameter. It appears the density of PANI particles increases with the increase of aniline quantity added. The PANI homopolymer globules prepared under the same condition were much smaller than 10–20 nm [42]. The present results are very different from the reports obtained by Bae, which state that the morphology changes from spherical particles to a non-particulate and uniform structure as the content of

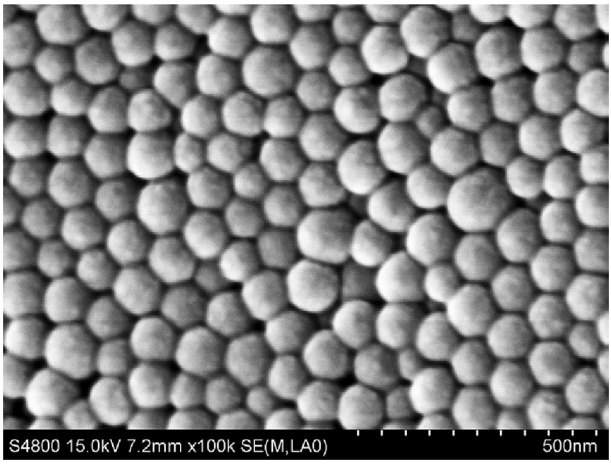

Fig. 3 SEM image of SA-PO latexes

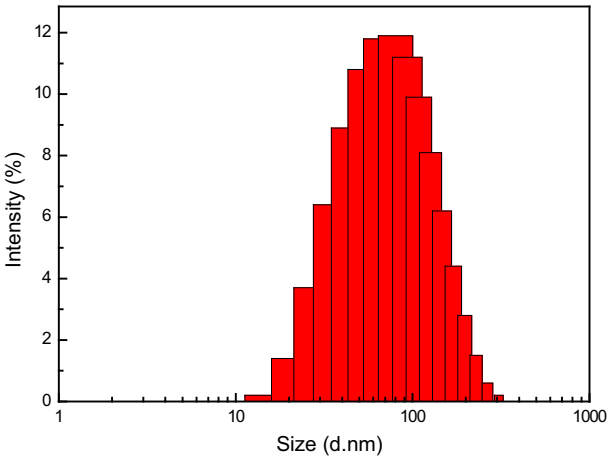

Fig. 4 Particle size distribution of SA-PO latexes

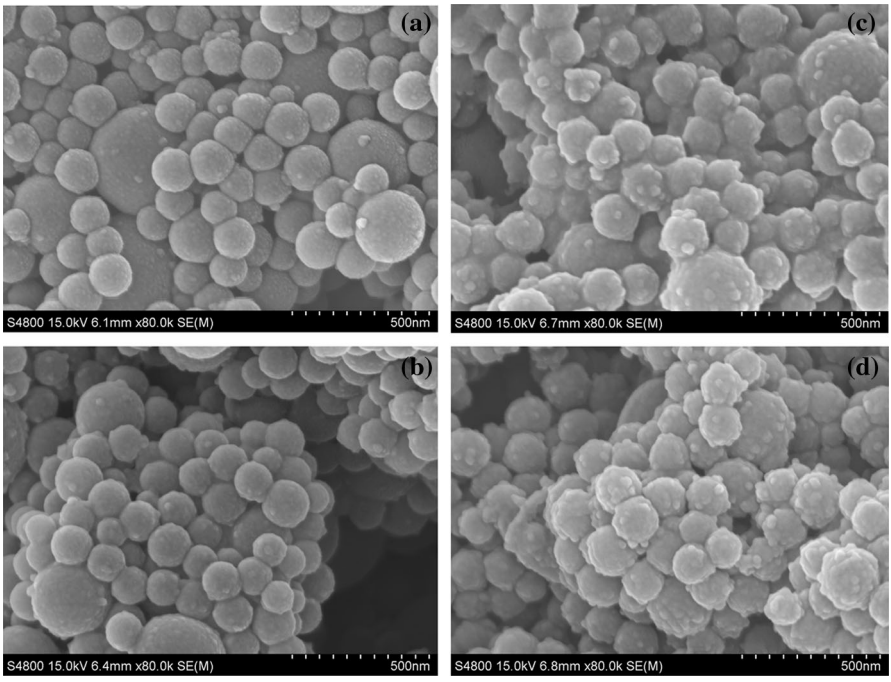

Fig. 5 SEM images of PANI-SA

PANI increases [43]. It is worth mentioning that there are almost no free and aggregated PANI observed. This is due to the electrostatic attraction between the aniline cation and negatively charged SA-PO particles (Scheme 1) and the hydrogen bonding driven by the interaction between the aniline N–H group and phosphate group [44].

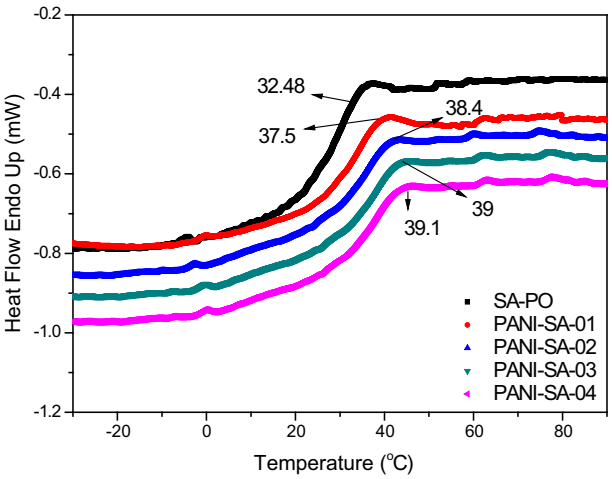

Fig. 6 DSC curves of SA-PO and PANI-SA

DSC analysis

Glass transition is a change similar to the second-order transition, but different from the first-order transition with phase transformations like crystallization or melting. Simultaneously, it follows a second-order thermodynamics with dH/dt changing discontinuously. From the perspective of molecular motion, glass transition applies to the micro-Browning movement. The molecular motion freezes at temperatures below T_g and after reaching T_g, the movement becomes more active. Figure 6 shows DSC spectra of SA-PO and PANI-SA latexes. There is only one glass transition temperature in all cases. T_g of PANI-SA is significantly higher than that of SA-PO (32.5 °C). T_g of PANI-SA-01 increases to 37.5 °C with PANI content of 1 wt%, which is very different from the PANI composites prepared by physical blending which exhibit no significant change in T_g [43]. This result suggests that PANI can significantly limit the chain movement of SA-PO molecules [45]. Moreover, the PANI layer bonded on the surface of SA-PO serves as the thermal barrier and inhibits the mobility of SA-PO polymer chains [45]. After further increasing PANI content, the T_g increases accordingly, but does not increase significantly, especially in the case of PANI-SA-03 and PANI-SA-04. From these results, it can be concluded that only the part of PANI that has bonded on SA can limit the chain movement of the SA molecule.

TGA

Thermogravimetric measurement is performed on samples to evaluate the thermal stability. The purpose of this is to observe the influence of each component of the composite on the mass loss with changing temperature. TGA of PANI-SA-01 and PANI-SA-02 were selected to be investigated and the results are shown in Fig. 7. The first thermal weightlessness took place around 100 °C, which is attributed to the

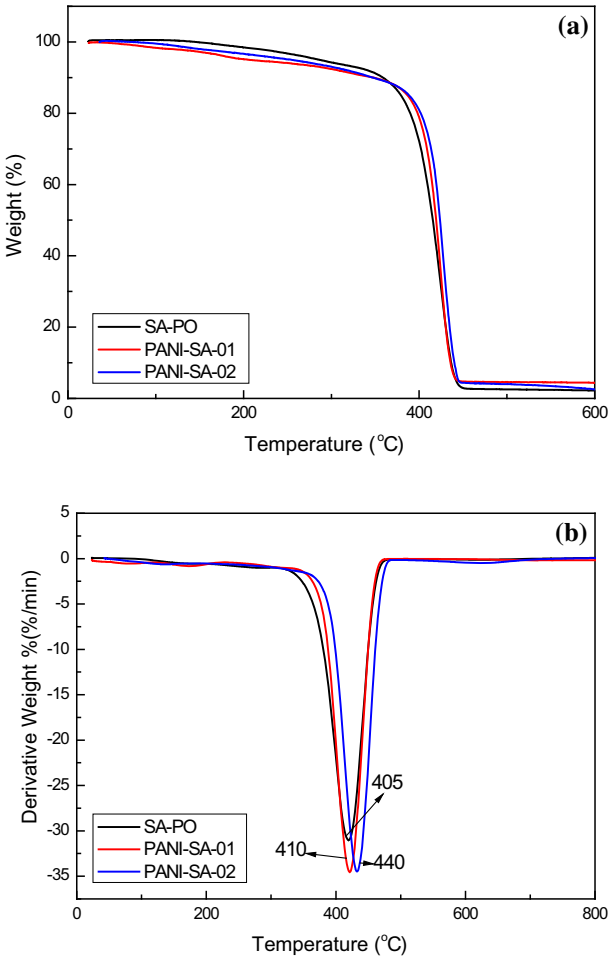

Fig. 7 TGA (**a**) and DTA (**b**) curves of SA-PO and PANI-SA

evaporation of residual water. More water weight loss took place for the PANI-SA-01 and PANI-SA-02 compared to SA-PO, which is mainly because of the strong hydrogen bonding interaction between PANI and water [44]. In the range of 150–250 °C, the decomposition of oligomers from the synthesis of SA-PO and volatilization of hydrochloric acid used for protonation can be observed. At 400 °C, there is a sudden mass loss in all the samples due to the decomposition of the matrix polymer chain. According to DTA spectra (Fig. 7b), the maximal thermal decomposition temperature of PANI-SA-01 is 10 °C higher than SA-PO. However, the maximal thermal decomposition temperature of PANI-SA-02 is not obviously enhanced compared to that of PANI-SA-01. The present results suggest that there is good interface adhesion between PANI and SA, and can increase the thermal stability of SA, which is different from the report that PANI can improve the thermal stability of a polymer matrix in its blending system [46].

Mechanical property of PANI-SA latex film

The tensile strength and elongation at break are shown in Fig. 8. Both the tensile strength and elongation at break increase with the increase of PANI in PANI-SA. Even when PANI content reaches 8 wt% in PANI-SA, the tensile strength and elongation at break are 99.2 MPa and 25.7 % respectively. This result indicates that the bonding of PANI has a positive effect on the mechanical properties of SA latex film. This excellent result is caused by the good distribution of PANI in PANI-SA latex film and by the good interfacial adhesion between PANI and SA latex.

Anti-corrosion performance of PANI-SA latex coating

Bode plots from EIS measurements conducted for the SA-PO and PANI-SA coated steel panels are shown in Fig. 9. The samples were immersed in 3.5 wt% NaCl saline at room temperature for 7 and 21 days. As seen in Fig. 9a, $|Z|_{0.1Hz}$ of pure SA coating at the immersion time of 7 days was 10^5 Ω. As the immersion time extended, $|Z|_{0.1Hz}$ decreased, and $|Z|_{0.1Hz}$ becomes 1.16×10^4 Ω after immersed for 21 days. However, as illustrated in Fig. 9b, $|Z|_{0.1Hz}$ of PANI-SA-02 (PANI content is 2wt %) at the immersion time for 7 and 21 days was 1.03×10^5 and 1.08×10^5 Ω respectively. When PANI content increases to 4 wt% (PAIN-SA-04), $|Z|_{0.1Hz}$ can maintain 1.87×10^5 Ω at the immersion time for 7 and 21 days. These results suggest that 2–4 wt% of PANI in SA-PANI can significantly improve the corrosion resistance performance of waterborne SA coating. This result is caused by either the formation of the passive film between metal and coating catalyzed by PANI or it is caused by the formation of a phosphate complex compound with PO_4^{3-} functional groups released from PANI-SA.

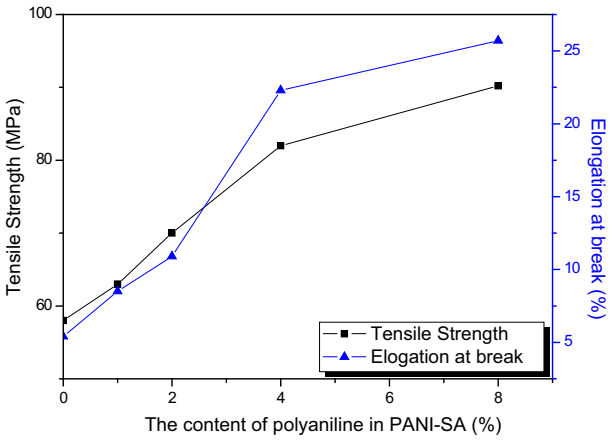

Fig. 8 The effect of polyaniline content on tensile strength and elongation at break of PANI-SA

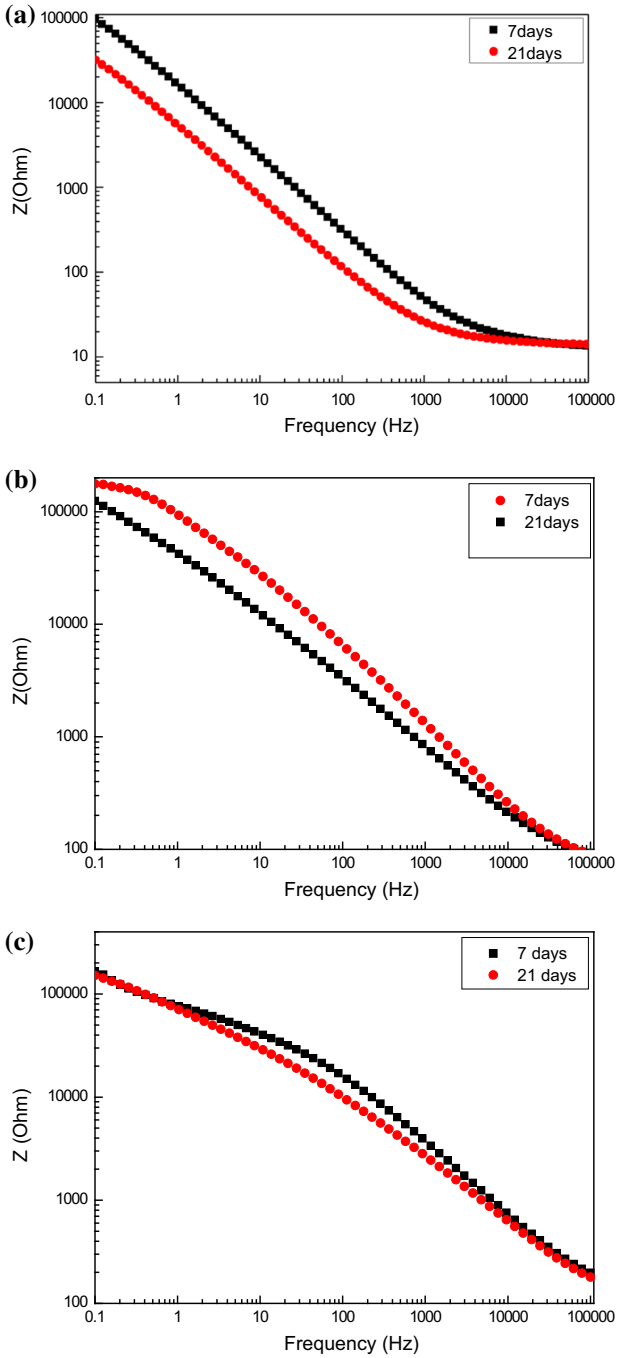

Fig. 9 Impedance plots for steel coated with SA-PO (**a**), PANI-SA-02 (**b**) and PANI-SA-04 (**c**)

Conclusions

In conclusion, PANI-SA composites were successfully prepared through in situ chemical oxidation polymerization of aniline on the surface of SA latexes. The small spherical PANI particles with 10–20 nm in diameter are bonded on the surface of SA latexes. The bonding of PANI on SA latexes results in increased T_g and the thermal stability of SA significantly. This composite can not only avoid the aggregation of PANI but also has good interfacial adhesion. The PANI can enhance the mechanical properties of SA latex film and improve the corrosion resistance performance of waterborne SA coating significantly.

Acknowledgments This research was financially supported by a grant from the University Science Foundation of Jiangsu province (No. 14KJA430006), Combination of innovative funding (No. SBY2014020171), through the Priority Academic Program Development of Jiangsu Higher Education Institutions and the Propulsion Engineering Program of Industrialization of Research Findings of Jiangsu Higher Education Institutions (JH10-42). The characterizations were conducted at the Testing Center of the Yangzhou University.

References

1. Hua MY, Hwang GW, Chuang YH, Chen SA (2000) Synthesis of β-iminoaminate zirconium complexes and their application in ethylene polymerization. Macromolecules 33:6235–6238
2. Hoffman K, Samuelsen E, Carlsen PJ (2000) Broken π-conjugated thiophene systems: 1. Synthesis and polymerization of 2,2′-di(alkylthienyl) methanes. Synth Met 113:161–166
3. Hong XY, Tyson JC (2000) Controlling the macromolecular architecture of poly(3-alkylthiophene)s by alternating alkyl and fluoroalkyl substituents. Macromolecules 33:3502–3504
4. Mengoli G, Munari MT, Bianco P, Musiani MM (1981) Anodic synthesis of PANI coatings onto fe sheets. J Appl Polym Sci 26:4247–4257
5. Iribarrenlaco JI, Villota FC, Mestres FL (2005) Corrosion protection of carbon steel with thermoplastic coatings and alkyd resins containing PANI as conductive polymer. Prog Org Coat 52:151–160
6. Albertsson A, Eklund M (1994) Synthesis of copolymers of 1,3-dioxan-2-one and oxepan-2-one using coordination catalysts. J Polym Sci Polym Chem 32:265–279
7. Shadi L, Karimi M, Entezami AA, Safa KD (2013) A facile synthesis of polyaniline/polyethylene glycol/polyaniline terpolymers: preparation of electrospun conducting nanofibers by blending of the terpolymers with polycaprolactone. Polym Bull 70:3529–3545
8. Wessling B (1997) Scientific and commercial breakthrough for organic metals. Synth Met 85:1313–1318
9. Sathiyanarayanan S, Muralidharan S, Venkatachari G (2005) Corrosion protection of steel by polyaniline (PANI) pigmented paint coating. Prog Org Coat 53:297–301
10. Popovic MM, Grgur BN, Miskovic-Stankovic VB (2005) Corrosion studies on electrochemically deposited PANI and PANI/epoxy coatings on mild steel in acid sulfate solution. Prog Org Coat 52:359–365
11. Pud AA, Shapoval GS, Kamarchik P (1999) Electrochemical behavior of mild steel coated by polyaniline doped with organic sulfonic acids. Synth Met 107:111–115
12. Wessling B (1994) Passivation of metals by coating with polyaniline: corrosion potential shift and morphological changes. Adv Mater 6:226–228
13. Epstein AJ, Smallfield JAO, Guan H (1999) Corrosion protection of aluminum and aluminum alloys by polyanilines: a potentiodynamic and photoelectron spectroscopy study. Synth Met 102:1374–1376
14. Torresi RM, Souza S, Silva JEPd (2005) Galvanic coupling between metal substrate and polyaniline acrylic blends: corrosion protection mechanism. Electrochim Acta 50:2213–2218
15. Kinlen PJ, Menon V, Ding YW (1999) A mechanistic investigation of polyaniline corrosion protection using the scanning reference electrode technique articles. J Electrochem Soc 146:3690–3695

16. Schauer T, Joos A, Dulog L (1998) Protection of iron against corrosion with polyaniline primers. Prog Org Coat 33:20–27
17. Musiani MM, Mengoli G, Furlanetto F (1984) Improved polyaniline coatings by in situ electropolymerization. J Appl Polym Sci 29:4433–4438
18. Kang ET, Neoh KG, Tan KL, Uyama Y, Morikawa N, Ikada Y (1992) Surface modifications of polyaniline films by graft copolymerization. Macromolecules 25:1959–1965
19. Ren L, Li K, Chen X (2009) Soft template method to synthesize polyaniline microtubes doped with methyl orange. Polym Bull 63:15–21
20. Ruckenstein E, Yang SJ (1993) An emulsion pathway to electrically conductive polyaniline-polystyrene composites. Synth Met 53:283–292
21. Li Y, Wang Z, Gu H, Xue G (2011) A facile strategy for synthesis of multilayer and conductive organo-silica/polystyrene/polyaniline composite particles. J Collid Interface Sci 355:269–273
22. Mehdi J (2013) Recent progress in chemical modification of polyaniline. Prog Polym Sci 38:1287–1306
23. Jaymand M (2011) Synthesis and characterization of novel type poly (4-chloromethyl styrene-graft-4-vinylpyridine)/TiO2 nanocomposite via nitroxide- mediated radical polymerization. Polymer 52:4760–4769
24. Chen Y, Kang ET, Neoh KG, Tan KL (2000) Chemical modification of polyaniline powders by surface graft copolymerization. Polymer 41:3279–3287
25. Hosseini SH (2006) Investigation of sensing effects of polystyrene-graft-polyaniline for cyanide compounds. J Appl Polym Sci 101:3920–3926
26. Wang Y, Shi Y, Xu X, Liu F, Yao H, Zhai G (2009) Preparation of PANI-coated poly (styrene-*co*-styrene sulfonate) nanoparticles in microemulsion media. Colloid Surf A Physicochem Eng Asp 345:71–74
27. Lu Q, Gao Y, Zhao Q, Li J, Wang X, Wang F (2013) Novel polymer electrolyte from poly(carbonate-ether) and lithium tetrafluoroborate for lithium–oxygen battery. J Power Sources 242:677–682
28. Chiou WC, Han JL, Lee SN (2008) Synthesis and studies of the physical properties of polyaniline and polyurethane-modified epoxy composites. Polym Eng Sci 48:345–354
29. Yang CY, Cao Y, Smith P (1993) Morphology of conductive, solution-processed blends of polyaniline and poly(methyl methacrylate). Synth Met 53:293–301
30. Talo A, Passiniemi P, Forsen O (1997) Polyaniline/epoxy coatings with good anti-corrosion properties. Synth Met 85:1333–1334
31. Banerjee P, Mandal BM (1995) Conducting polyaniline nanoparticle blends with extremely low percolation thresholds. Macromolecules 28:3940–3943
32. Banerjee P, Bhattacharyya SN, Mandal BM (1995) Poly(vinyl methyl ether) stabilized colloidal polyaniline dispersions. Langmuir 11:2414–2418
33. Stejskal J, Spirkova M, Riede A, Helmstedt M, Mokreva P, Prokes J (1999) Polyaniline dispersions 8. The control of particle morphology. Polymer 40:2487–2492
34. Landfester K (2001) The generation of nanoparticles in miniemulsions. Adv Mater 10:765–768
35. Antonietti M, Landfester K (2002) Polyreactions in miniemulsions. Prog Polym Sci 27:689–757
36. Liu W, Kumar J, Tripathy S, Senecal KJ, Samuelon L (1999) Enzymatically synthesized conducting polyaniline. J Am Chem Soc 121:71–78
37. Arsalani N, Hayatifar M (2005) Preparation and characterization of novel conducting polyaniline–perlite composites. Polym Int 54:933–938
38. Tsotra P, Friedrich K (2004) Thermal, mechanical, and electrical properties of epoxy resin/polyaniline-dodecylbenzenesulfonic acid blends. Synth Met 143:237–242
39. Huang WS, MacDiarmid AG (1993) Optical properties of polyaniline. Polymer 34:1833–1845
40. Xia Y, Wiesinger JM, MacDiarmid AG, Epstein AJ (1995) Camphorsulfonic acid fully doped polyaniline emeraldine salt: conformations in different solvents studied by an ultraviolet/visible/near-infrared spectroscopic method. Chem Mater 7:443–445
41. Kim B, Oh S, Han M, Im S (2002) Preparation of PANI-coated poly (styrene-*co*-styrene sulfonate) nanoparticles. Polymer 43:111–116
42. Jiang L, Cui Z (2006) One-step synthesis of oriented polyaniline nanorods through electrochemical deposition. Polym Bull 56:529–537
43. Bae WJ, Jo WH, Park YH (2003) Preparation of polystyrene/polyaniline blends by in situ polymerization technique and their morphology and electrical property. Synth Met 132:239–244
44. Ruckenstein E, Yuan Y (1998) Colloidal scale blends of poly(*p*-benzamide) with sulfonated polystyrene and poly(vinyl acetate). Polymer 39:1043–1049

45. Davodi B, Lashkenari MS, Esiazadeh H (2011) Colored nanoparticles dispersions as electronic inks for electrophoretic display. Synth Met 161:1270–1275
46. de Farias RF, Nunes LM (2002) Scales of basicity based on thermochemical data of adducts. J Therm Anal Calorim 67:579–587